External Load-Based Sensing of Electrical Current Degradation in Industrial Robots

Vinh Nguyen
Intelligent Systems Division
National Institute of Standards and Technology
Gaithersburg, MD, USA
vinh.t.nguyen@nist.gov

Jeremy Marvel
Intelligent Systems Division
National Institute of Standards and Technology
Gaithersburg, MD, USA
jeremy.marvel@nist.gov

2021 IEEE Sensors | 978-1-7281-9501-8/21/$31.00 ©2021 IEEE | DOI: 10.1109/SENSORS47087.2021.9639250

***Abstract*—Industrial robotic arms are used extensively in sectors including manufacturing, healthcare, and infrastructure. Electrical current sensors located in the joints of industrial robots are critical for maintaining safe and optimal performance. However, the current sensors are subject to inaccuracies resulting from performance degradation, which results in safety hazards and sub-optimal performance. Thus, this research describes, develops, and experimentally validates an external load-based sensing system and methodology to detect unacceptable drift of current sensors in industrial robots. The initial states of the current sensors are recorded using low-cost load cells mounted on each joint of a UR10 robot. Thus, subsequent current sensor measurements can be compared to the initial state to determine statistically significant current degradation. This paper demonstrates the load-based sensing system is subject to less variability compared to current sensor verification under free loading conditions, and further analysis shows the load cells can be selectively mounted onto specific joints. In addition, a case study shows that the external load-based system can robustly detect simulated current sensor degradation. Thus, this sensing system is an efficient, robust, and cost-effective method towards detecting electrical current degradation in industrial robots.**

***Keywords*—degradation; sensor systems; load cell; industrial robot systems; verification; monitoring and diagnostics**

I. Introduction

Autonomous industrial robots are equipped with sensors to monitor the electric current in each motor housed in each joint. Robot manufacturers use these current sensors in their industrial robots for safety-related force-limiting [1], end effector gravity compensation [2], and compliant teach-point programming [3]. In addition, researchers have also used the electrical current sensors for applied force estimation [4]. Thus, current sensors are critical for industrial robots to conduct tasks safely while maintaining optimal performance.

However, the angular and current sensor accuracies of industrial robots are known to degrade due to repeated metallurgical impact [5]. Thus, recent research has been conducted towards developing sensing systems for monitoring and detecting robot degradation. However, most of prior research is focused on positional accuracy. For example, physical detection systems [6] and vision systems [8] have been used to detect positional accuracy degradation. Because electrical current sensors are known to experience lifetime drift as high as 5.7% [9], degradation in current sensors can impact the safety and force sensing characteristics of industrial robots. Since the robot's currents are recorded internally, accessing raw sensor values is difficult via external means and is dependent on the robot's self-reporting. Therefore, the current sensors are viewed as gray boxes in which the robot's internal states and the reported states are subject to uncertainty. Thus, there is a need for sensing systems for electrical current sensor verification.

This paper presents a low-cost, straightforward, and efficient external load-based system to monitor electrical current sensor degradation of a Universal Robot UR10 robot. The robot is driven to a pose that applies force to each of the load cells mounted on each of the joints. Electrical current readings are then recorded for initial state qualification. Thus, when the robot conducts its operations, it can periodically drive to the same pose as the initial state qualification for verification. The performance of the described sensing system is experimentally compared to conducting current sensor verification in a pose with no load (free load). In addition, the sensing system is applied to a case study where a known degradation in current is applied. Results of the analysis are discussed followed by conclusions and recommendation for future work.

II. Theory and Approach

A brief description of the load-based monitoring system shown in Fig. 1 is provided in this section. The specific load cell implementation is described followed by initial state qualification and verification procedures.

A. Load Cell Setup

As shown in Fig. 1, a TAL220B strain-based load cell was mounted onto each robot joint. The load cell was fastened onto an additively manufactured mount that was adhered onto the robot joint using Loctite 454. In addition, a hard stop was mounted onto the connecting link. Thus, a force is experienced by the load cell when a joint rotates the hard stop into the sensor. Hence, the resulting strain in the load cell changes the resistance in the internal bridge circuit. When an excitation voltage is applied, the measured voltage across the bridge circuit will change linearly to the applied force. Each load cell was calibrated by applying a nominal 9.81 N load and recording the linear gain between the load cell and applied load. However, note that repeatability is more critical than

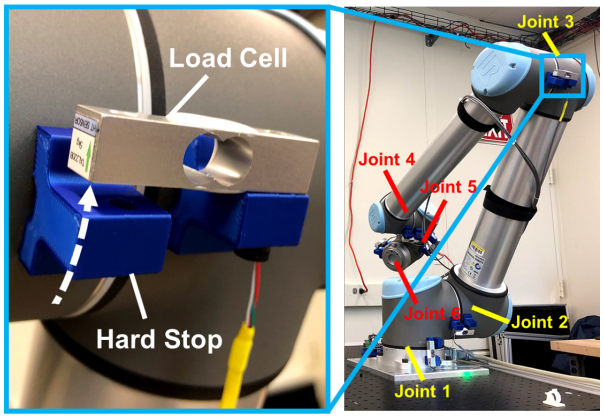

Fig. 1. Joint 3 load cell setup at the initial qualification pose.

calibration since the sensor system compares present sensor readings to an initial state. The load cells were each connected to a SparkFun Qwiic Scale, which host the NAU7802 Analog-to-Digital Converter (ADC). The Qwiic Scales supplied the excitation voltage to the load cells and transmitted voltage readouts via Inter-Integrated Circuit (I^2C) communication. Because the Qwiic Scales shared I^2C addresses, the boards were connected to a SparkFun Qwiic Mux Breakout to resolve I^2C devices sharing the same address. The Qwiic Mux Breakout was connected to a Arduino Uno microcontroller variant (SparkFun RedBoard) via I^2C, and the RedBoard was connected to a computer via USB serial. The schematic of the communication architecture is shown in Fig. 2 (top).

B. Initial State Qualification

The sensing system in this paper requires an initial state for subsequent verification. In this work, the pose for verification is shown in Fig. 1. The angles of Joints 1...6 for this pose are $[-180.5°, -53.5°, -152.5°, -110.0°, 153.0°, -153.5°]$. After the robot reaches its pose, each current sensor is qualified by rotating each joint at a fixed velocity (0.1°/sec in this work) towards its load cell. The load cell will output a nonzero load value due to interference with the hard stop, and the rotation stops when the load exceeds a threshold (15 N in this work). The average of 200 current sensor readings provided by the UR10 controller are recorded. Thus, this reading is used to establish baseline control limits for fault detection. This step is repeated for each joint multiple times to calculate mean and standard deviation values for statistical control charts.

C. Verification

After initial state qualification is conducted, the robot can conduct its intended operation. When the current degradation requires checking, the robot simply moves to the pose used in the initial state qualification. The loading procedure is conducted, and the current sensor reading of each joint is recorded. The current sensor reading is then compared to either a predetermined acceptable threshold based on task performance or to statistical control charts. Thus, this method is simple for end-users to conduct and robust to uncertainties. The process flow is shown in Fig. 2 (bottom).

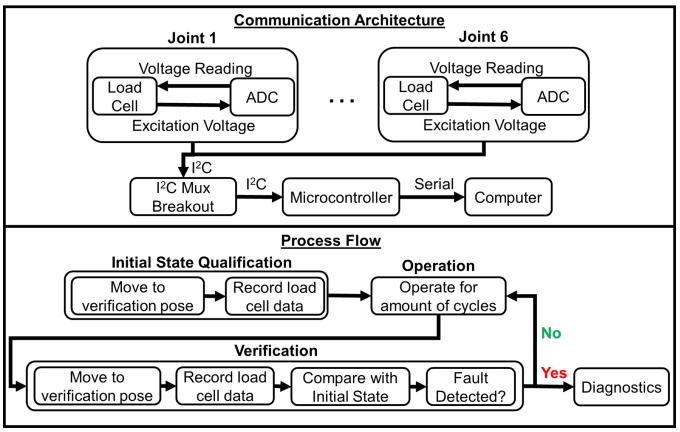

Fig. 2. Communication architecture (top) and process flow (bottom).

III. Experimental Setup

An alternative approach would be to record current sensor readings at a predetermined pose without applying external load (free loading) to establish a baseline recording. Verification would then be conducted by returning to the initial pose without the load cells. Thus, the external load-based system is compared to the free loading condition where the free loading pose is the pose in Fig. 1 before applying the load.

For initial state qualification, the UR10 is driven to the pose in Fig. 1. Five measurements each are collected for the sensor system and free loading condition to determine the mean and standard deviation used for the statistical control charts. In this work, a 3-Sigma Control Chart [10] is used to establish the Upper Control Limits (UCL) and Lower Control Limits (LCL). However, in alternative implementations, the acceptable range can be determined based on task and safety requirements.

Then, an operation by the UR10 is conducted with the start pose shown in Fig. 3 with joint angles of $[-90°, -90°, -90°, 0°, 90°, 0°]$ The joints are moved by 5° (end pose in Fig. 3) and retracted 50 times at 10°/sec. Then the UR10 is driven back to Fig. 1 where recordings are taken for free loading and external loading conditions. Studies of current degradation in industrial robots are limited; so the current degradation is simulated to increase by 20 mA and 10 mA for Joints 1, 2, and 3, and Joints 4, 5, and 6, respectively, per operation sequence. Note that the simulated drift is assumed to be the only source of degradation in these experiments.

IV. Results

This section discusses the experimental results.

A. Initial State Qualification

Table I shows the normalized standard deviations of each joint's current sensor measurements during initial state qualification. Table I shows that the external load-based system exhibits less normalized standard deviation than the free loading approach. Thus, the external load-based sensing system

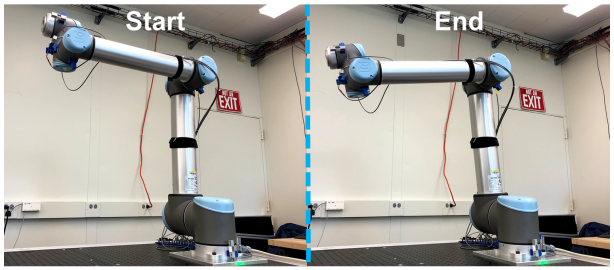

Fig. 3. Start (left) and end (right) poses for operating motion.

improves the consistency of the current sensing measurements. This is because the external load-based system applies a preload that can be consistently used for the current sensors while the free loading approach is subject to hysteresis.

However, note that Joint 2 does not show as much consistency improvement. To understand the reasoning behind this result, a power relationship was fitted between the normalized standard deviation and the average current in the free loading condition resulting in a clear power relationship of $0.065Ave^{-0.75}$ with a correlation coefficient of 0.95. Since the current is correlated to the experienced torque, this analysis shows that recording the current in free loading conditions is acceptable in positions that experience less torque, such as Joint 2 in these experiments. Thus, a more efficient hybrid approach can be conducted where the external load cells are mounted only on the joints that do not experience much torque.

TABLE I
INITIAL QUALIFICATION AVERAGE AND NORMALIZED STANDARD DEVIATION OF CURRENT SENSORS (AMP) FOR FREE LOADING VS. EXTERNAL SENSOR-BASED CONDITIONS.

		Joint Number					
		1	**2**	**3**	**4**	**5**	**6**
Ave.	**Free**	-0.88	-0.20	2.74	0.07	0.21	0.02
	Sensor	-1.07	-0.07	2.76	-0.07	0.25	-0.26
Std. Dev.	**Free**	0.07	0.20	0.04	0.29	0.19	2.19
	Sensor	0.04	0.19	0.01	0.13	0.07	0.06

B. Verification

Fig. 4 shows the results of the verification case study with the simulated drift. All joints show that the external load-based sensing system has closer control limits than the free loading condition. This is because the standard deviation of the free loading condition is larger, which corresponds to larger control limits to reduce the occurrence of false alarms. However, note that the free loading results in certain joints, including Joint 1 and 3, are prone to more variation and false alarms. In addition, there are multiple cases in free loading, such as Joints 5 and 6, where the drift is not detected within the 10 operations.

The external load-based sensing system readings are shown to linearly increase with operation, which is expected as the drift is introduced. In addition, the increase in the sensing

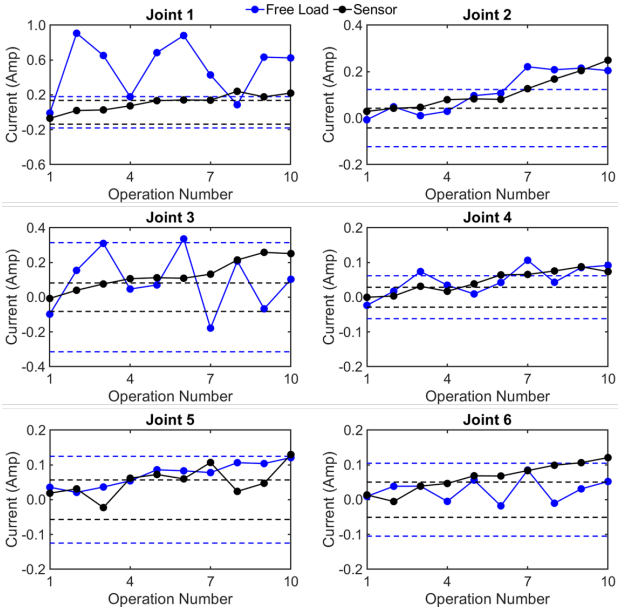

Fig. 4. Control charts for verification. All values and control limits are shifted by the average of the UCL and LCL (represented by dashed lines.

measurements appears to be less noisy than the free loading condition. Thus, the results in Fig. 4 show that the external load-based system can detect current degradation faster than the free loading approach due to more consistent measurements. Hence, the external load-based system is a simple and cost-effective method to detect current sensor degradation.

V. CONCLUSIONS

An external load-based sensing system for detecting current sensor degradation in industrial robots was described and experimentally validated. This sensing system is intended to provide a cost-effective solution for end users to introduce periodic checks for the current sensors in industrial robots. In addition, this work can be used for compensation, estimating remaining useful life, and maintenance scheduling through periodic checks.

However, this approach restricts the robot workspace in addition to not directly measuring current. Thus, future work involves using direct electrical current sensors for direct comparison, especially when not in free-loading conditions. Such an approach can be used to verify electrical current sensors for both in-situ accuracy and degradation.

ACKNOWLEDGMENT

This work was funded by NIST and the National Research Council Research Associateship Program.

DISCLAIMER

Certain commercial equipment, instruments, or materials are identified in this paper in order to specify the experimental procedure adequately. Such identification is not intended to imply recommendation or endorsement by NIST, nor is it intended to imply that the materials or equipment identified are necessarily the best available for the purpose.

REFERENCES

[1] P. Aivaliotis, S. Aivaliotis, C. Gkournelos, K. Kokkalis, G. Michalos, and S. Makris, "Power and force limiting on industrial robots for human-robot collaboration," Robot. Comput. Integr. Manuf., vol. 59, pp 346-360, October 2019.

[2] V. Arakelian, "Gravity compensation in robotics," Adv. Robot., vol. 30, no. 2, pp 79-96, November 2015.

[3] J. Fernández, D. Mronga, M. Günther, T. Knobloch, M. Wirkus, M. Schröer, M. Trampler, S. Stiene, E. Kirchner, V. Bargsten, T. Bänziger, J. Teiwes, T. Krüger, and F. Kirchner, "Multimodal sensor-based whole-body control for human–robot collaboration in industrial settings," Rob. Auton. Syst., vol. 94, pp 102-119, August 2017.

[4] A. Wahrburg, J. Bös, K. D. Listmann, F. Dai, B. Matthias and H. Ding, "Motor-current-based estimation of Cartesian contact forces and torques for robotic manipulators and its application to force control," IEEE Trans. Autom. Sci. Eng., vol. 15, no. 2, pp. 879-886, April 2018.

[5] G. Qiao and B. Weiss, "Accuracy degradation analysis for industrial robot systems," Int. Manu. Sci. Eng. Conf., June 2017.

[6] B. Weiss and J. Kaplan, "Assessment of a novel position verification sensor to identify and isolate robot workcell health degradation," J. Manu. Sci. Eng., vol. 143, no. 4, pp 041008, November 2020.

[7] R. Algburi and H. Gao, "Health assessment and fault detection system for an industrial robot using the rotary encoder signal," Energies, vol. 12, no. 14, pp 2816, July 2019.

[8] U. Izagirre, I. Andonegui, L. Eciolaza, and U. Zurutuza, "Towards manufacturing robotics accuracy degradation assessment: A vision-based data-driven implementation," Robot. Comput. Integr. Manuf., vol. 67, pp. 102029, July 2020.

[9] ACS71240 Datasheet (2020). Accessed: April 9, 2021. [Online]. Available: https://www.allegromicro.com/-/media/files/datasheets/acs71240-data-sheet.ashx, 2020.

[10] K. Govindaraju and C. La, "Run Length Variability and Three Sigma Control Limits," Econ. Qual. Cont., vol. 19, no. 4, pp 175-184, March 2010.